

Article

# Large-Area Coating of Previtamin D<sub>3</sub> Based on Roll-to-Roll Processing

Janghoon Park <sup>1,†</sup>, Yoonki Min <sup>1,†</sup>, Jongsu Lee <sup>1</sup>, Hakyung Jeong <sup>1</sup>, Youngwook Noh <sup>1</sup>, Kee-Hyun Shin <sup>2</sup> and Dongjin Lee <sup>2,\*</sup>

<sup>1</sup> Department of Mechanical Design and Production Engineering, Konkuk University, 120 Neungdong-ro, Gwangjin-gu, Seoul 05029, Korea; janghoonpark2@gmail.com (J.P.); youngi032457@gmail.com (Y.M.); ljs8755@gmail.com (J.L.); greenihk92@gmail.com (H.J.); kiwonno2@gmail.com (Y.N.)

<sup>2</sup> School of Mechanical Engineering, Konkuk University, 120 Neungdong-ro, Gwangjin-gu, Seoul 05029, Korea; khshin@konkuk.ac.kr

\* Correspondence: djlee@konkuk.ac.kr; Tel.: +82-2-450-0452

† These authors contributed equally to this work.

Received: 22 August 2019; Accepted: 9 September 2019; Published: 11 September 2019



**Abstract:** We propose a roll-to-roll process for vitamin D<sub>3</sub> patch production. A solution of 7-dehydrocholesterol is applied to a plastic film by roll-to-roll slot-die coating and dried by a far-infrared lamp. Upon exposure to ultraviolet B irradiation, these films are converted to previtamin D<sub>3</sub> films. After heat-treating the previtamin D<sub>3</sub> film, high-performance liquid chromatography measurements are performed using commercial vitamin D<sub>3</sub> as a standard sample. The results confirm that vitamin D<sub>3</sub> can be produced by large-area coating and post-treatment processes. Specifically,  $3.16 \pm 0.746$  mg of vitamin D<sub>3</sub> is obtained through ultraviolet B irradiation and heat-treatment of  $24.8 \pm 1.44$  mg of coated 7-dehydrocholesterol.

**Keywords:** slot-die coating; roll-to-roll (R2R); vitamin D<sub>3</sub>; ultraviolet B (UVB); high-performance liquid chromatography (HPLC)

## 1. Introduction

In recent years, lack of vitamin D<sub>3</sub> in humans worldwide has become a real problem. In fact, it is estimated that approximately one billion people suffer from vitamin D<sub>3</sub> deficiency due to less photosynthesis with certain skin types, aging, and scarce exposure to sunlight [1]. Vitamin D<sub>3</sub> plays a major role in developing and maintaining the ossified skeleton by stabilizing the blood calcium level within the normal range [2]. Moreover, vitamin D<sub>3</sub> deficiency can cause several diseases such as cancer, diabetes, hypertension metabolic syndrome, and other autoimmune and infectious diseases [3].

Vitamin D<sub>3</sub> is synthesized in the human body through exposure to sunlight (specifically, ultraviolet B (UVB) radiation, 290–315 nm) and dietary intake. The daily recommended dose of vitamin D<sub>3</sub> is 10 µg; however, considering that egg yolk has 10 µg of vitamin D<sub>3</sub> per 100 g and fish oil has 5–10 µg per 100 g, this dose cannot realistically be met via synthesis through food [4]. The most effective method to meet this dose is vitamin D<sub>3</sub> synthesis from UVB irradiation. However, UVB exposure risks DNA damage that is a major factor in the development of skin cancer [5]. Furthermore, vitamin D<sub>3</sub> deficiencies could also be caused by low UVB exposure during winter and the lack of sunshine in certain areas with polar nights [6]. Thus, although vitamin D<sub>3</sub> is mainly obtained through UVB exposure, this approach has some practical problems.

In this study, we introduce a novel previtamin D<sub>3</sub> patch containing 7-dehydrocholesterol (7-DHC) that produces vitamin D<sub>3</sub> under UVB exposure [7]. We also introduce a new approach for mass-producing such patches through a roll-to-roll (R2R) process. Conventional advanced R2R

processes [8] are used for producing electrical devices such as transistors, sensors, and solar cells using materials such as conductors, semiconductors, and insulators. To the best of our knowledge, no study has applied R2R processes to the production of biomaterials. The coating and post-treatment approaches proposed in this study for composite films of a polymer and vitamin D<sub>3</sub> materials will open new prospects in the fields of bio- and green-manufacturing.

## 2. Results and Discussion

The vitamin D<sub>3</sub> formation mechanism is based on the transformation of D-dosimeters [9]. A D-dosimeter is an *in vitro* model of vitamin D that measures the photodamage of DNA molecules following exposure to UVB radiation in the UV spectrum. 7-DHC, the provitamin D<sub>3</sub> used in this study, absorbs UVB radiation and converts to previtamin D<sub>3</sub> via the opening of its hexadiene ring, as shown in Figure 1a. Then, the obtained previtamin D<sub>3</sub> converts to vitamin D<sub>3</sub> via thermal isomerization with an intramolecular H shift. Nevertheless, Jacobs and Havingnga reported side photoconversion of three isomers from previtamin D<sub>3</sub>: lumisterol, toxysterol and tachysterol [10]. These conversions can be seen in the UV absorption spectra [11].

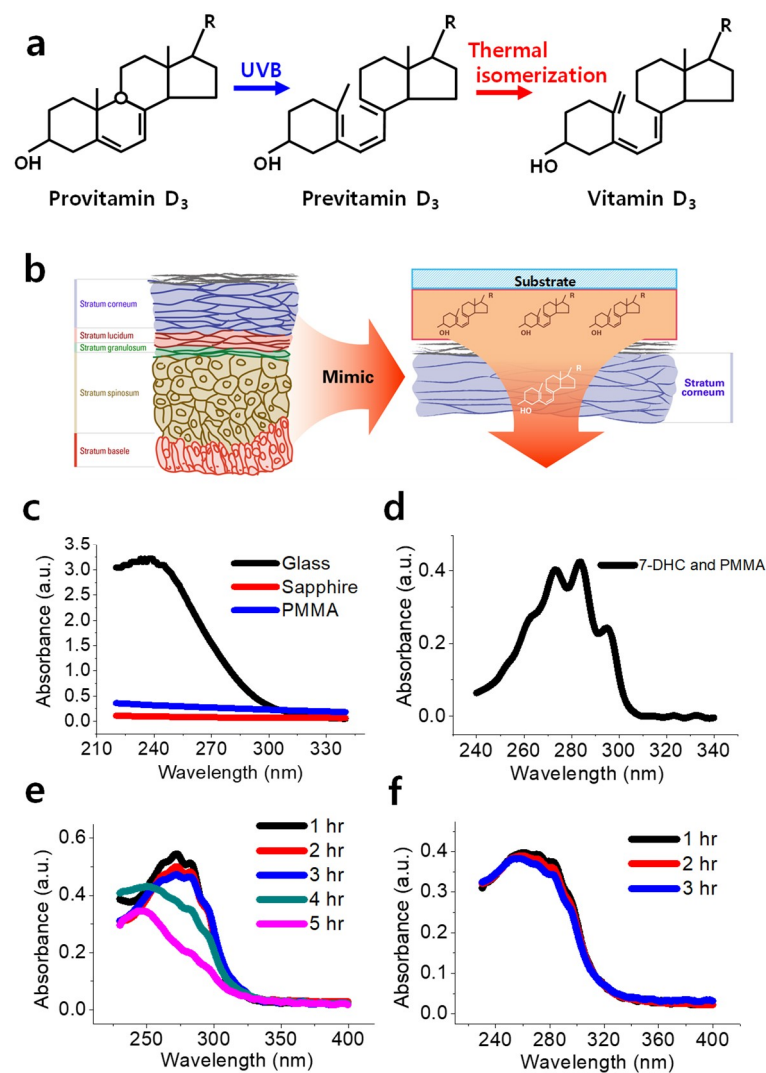


**Figure 1.** Concept and basic experimental results of this study. (a) The vitamin D<sub>3</sub> formation mechanism involves converting provitamin D<sub>3</sub> to previtamin D<sub>3</sub> through ultraviolet B (UVB) irradiation and then converting previtamin D<sub>3</sub> to vitamin D<sub>3</sub> by thermal isomerization [9]. (b) The conversion mechanism

of D-dosimeters in human skin is mimicked using V-Skin for the patch-type conversion of 7-dehydrocholesterol (7-DHC) to previtamin D<sub>3</sub> by UVB irradiation. (c) Absorbance spectra of glass, sapphire, and poly (methyl methacrylate) (PMMA)-coated sapphire. UV absorption of the glass substrate is not suitable for the base substrate owing to the high absorption characteristics below 300 nm. (d) The absorbance spectra of films mixed with 7-DHC and PMMA. Significant peaks at 261, 273, 283, and 295 nm correspond to 7-DHC. (e) Changes in absorbance spectra of 7-DHC/PMMA films exposed to UVB radiation for 1 to 5 h. After 4 to 5 h, a peak shift of 270 to 250 nm appears, demonstrating the formation of previtamin D<sub>3</sub>. (f) Changes in absorbance spectra when heated from 40 °C for 3 h. Vitamin D<sub>3</sub> does not appear at the absorption peak.

Human skin comprises an inner layer (dermis) and an outer layer (epidermis). The epidermis consists of five strata, as shown in Figure 1b: the stratum corneum, stratum lucidum, stratum granulosum, stratum spinosum, and stratum basele [12]. The two innermost strata, namely, the stratum spinosum and stratum basele, are known to contain a high concentration of 7-DHC.

In this study, we mimic the biomechanism of the epidermis by developing a polymer-mixed previtamin D<sub>3</sub> layer on a flexible polyethylene terephthalate (PET) substrate that can serve as a vitamin D<sub>3</sub> patch under UVB irradiation (Figure 1b). We call this product V-Skin. Then, the coated 7-DHC and polymer layer on the PET substrate was exposed to UVB radiation in the laboratory. V-Skin has a previtamin D<sub>3</sub> layer on the PET substrate, which is the preceding dosimeter of vitamin D<sub>3</sub>. V-Skin can be attached to the human body and can produce vitamin D<sub>3</sub> via thermal isomerization induced by body heat (Figure 1b).

Figure 1c shows the absorbance spectra of sapphire, PMMA-coated sapphire, and glass. Sapphire glass was used as the base substrate owing to its clear absorbance spectra at UV wavelengths. In contrast, the glass substrate showed a relatively high absorbance rate in the desired ranges, making it unsuitable for use as a base substrate. Further, the PMMA-coated sapphire substrate showed an increase in absorbance rate up to 0.359, however, it did not show significant peak changes in the wavelength range of 220–340 nm. Finally, the coated layer with 7-DHC and PMMA showed clear peaks at 261, 273, 283, and 295 nm that corresponded to 7-DHC, as shown in Figure 1d. Galkin and Terenetskaya reported the shift and change in absorbance peaks from 7-DHC to previtamin D<sub>3</sub> [9]. Figure 1e shows the transformation of the absorption spectrum of 7-DHC under UVB irradiation for a few hours. The four peaks in the absorbance spectra shifted from 270 to 250 nm and gradually disappeared after 4–5 h of UVB exposure; this verified the presence of previtamin D<sub>3</sub> and was consistent with the plateau changes reported by Galkin and Terenetskaya [9]. Lastly, the obtained previtamin D<sub>3</sub> was treated at 40 °C for 1–3 h, as shown in Figure 1f. However, no specific change was seen. This suggested that the optical measurement does not confirm vitamin D<sub>3</sub> production as reported in previous studies [9,13].

The previtamin D<sub>3</sub> film can be upscaled by an R2R manufacturing process [14]. The R2R system comprises numerous rollers linked by a flexible substrate (web) [15]. Figure 2a shows the proposed fabrication scheme that consists of the following three steps: R2R slot-die coating of synthesized solution, far-infrared (FIR) drying for solvent evaporation, and UVB irradiation for converting 7-DHC to previtamin D<sub>3</sub>. UVB irradiation was conducted offline using a UVB lamp owing to equipment limitations. The R2R system (SND Corporation Co., Ltd., Incheon, Korea) used in the study included an unwinder, outfeeder, offset pivot guider, dancer, load cell (L/C), FIR dryer, accumulator, proportional-integral-derivative (PID) controller, outfeeder, and rewinder, as shown in Figure S1.

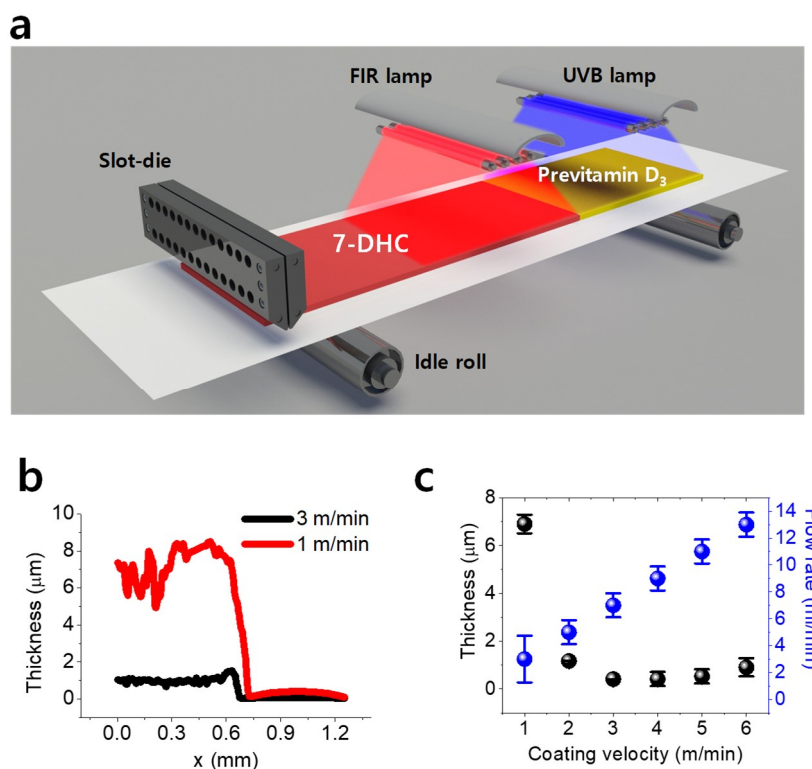


**Figure 2.** Roll-to-roll (R2R) process for continuous processing of previtamin D<sub>3</sub>. (a) A schematic diagram of the R2R process concept, including slot-die coating of 7-DHC/PMMA films, far-infrared (FIR) drying, and UVB post-treatment for conversion to previtamin D<sub>3</sub> (The UVB process was performed offline in this study). (b) Film thickness control through velocity change. (c) Change in coating film thickness with coating speed and flow rate control.

The process conditions of slot-die coating can be used to control the thickness of the coated layer and thereby increase the yield rate of previtamin D<sub>3</sub>. The dominant parameters affecting the thickness are known to be the liquid viscosity, liquid surface tension, liquid solid content, coating velocity, flow rate, and coating gap [16]. In this experiment, the capillary number is higher than 0.02 owing to the use of PMMA with an 18% concentration in the coating solution; therefore, the coating window is inappropriate for the use of the viscocapillary model [17]. Moreover, the minimum thickness can be obtained only by using a vacuum box in the system, and the general large-area coating machine does not have a vacuum box. Therefore, the wet thickness is always greater than the estimated thickness. To obtain a predictable thickness when using a high-viscosity solution without a vacuum box, the thickness can be predicted based on the mass conservation law, as shown in Equation (1) [18,19]:

$$t_{dry} = \frac{f_r}{nwV} \cdot \frac{\rho_l}{\rho_s} \quad (1)$$

Here,  $t_{dry}$ ,  $f_r$ ,  $n$ ,  $w$ ,  $V$ ,  $\rho_l$ , and  $\rho_s$  denote the dry thickness of a coated layer, flow rate, number of coating strips, width of a coating strip, coating velocity, density of the solid in a liquid, and density of the solid in a dried film, respectively. The coating velocity and flow rate were selected as process parameters in this study. Table S1 summarizes the operation conditions of the R2R slot-die coating process. The estimated thickness was in the range of 2–7  $\mu\text{m}$ , and it decreased with increasing speed, as shown in Figure S1. The flow rate conditions for a coating width of 130 mm affected the thickness reduction at high speed.

Figure 2b shows the measured thickness of the coated layer under coating velocities of 1 and 3 m/min. The corresponding obtained coated layer thicknesses were 6.9 and 0.4  $\mu\text{m}$ , respectively. The surface morphology of the coated layer with coating velocity of 3 m/min was better than that with

one of 1 m/min. Generally, a uniform coated surface is obtained at high speed [20]. Furthermore, all experimental results (Figure 2c) indicated that the coated layer thickness decreased with increasing coating speed; this agrees with the estimated result shown in Figure S2. However, unexpectedly, the thickness variation at low speeds remained stable because the meniscus was stable in a high-viscosity liquid [21].

The previously tested sapphire glass is rigid; therefore, it was replaced with a PET film. However, when PMMA and 7-DHC were coated on the PET film, the absorbance of the UV region varied greatly, as shown in Figure 3a. This is due to the high absorbance of the PET film at UV wavelengths (see Figure S3) [22]. When the absorbance is measured, scattering occurs in the PET film when UV light passes from the dispenser to the detector. In the R2R-based experiment, all conditions were set the same as those in the previous lab-scale experiment, and the amount of vitamin D<sub>3</sub> on the films was quantified using high-performance liquid chromatography (HPLC) measurements [23]. A window with dimension of 120 mm × 30 mm was cut in the rewind roll to allow UVB irradiation of the 7-DHC and PMMA film. The samples were exposed under a UVB lamp in a darkroom for 5 h, which is the optimal condition shown in Figure 1e. After exposure, the samples were heated at 40 °C for 2 h following the conditions recommended by Galkin and Ternetskaya [9]. The coated film should be in the liquid state for HPLC measurement; therefore, the PMMA film was immersed in toluene to separate it from the PET substrate and then dissolved by stirring. Finally, commercial oral vitamin D<sub>3</sub> (Solar D liquid 400, 0.278 mg/mL, Viva Pharmaceutical Inc., Richmond, BC, Canada) liquid was used as a standard calibration curve for the peak area as a concentration of the standard sample, as shown in Figure 3b (see Figure S4 and Table S2 for a photograph of the prepared samples and HPLC of commercial vitamin D<sub>3</sub>, respectively). The calibration curves were obtained for each experiment. “Low” was measured for low-thickness samples (thickness: 0.7 μm) and “High,” for high-thickness samples (thickness: 6.9 μm). Further, the dilution rate was doubled for high-thickness samples. The equations of the fitted curves for the “High” and “Low” sets are  $y = 35.0675x + 65.7071$  and  $y = 19.8042x + 3.6455$  ( $y$ : area,  $x$ : concentration), respectively. Figures S5a and S6a show the HPLC data of the standard sample in each experiment. As expected, the peak of the standard sample did not appear in the HPLC result of the coating film without UVB exposure (Figure 3c). Table 1 lists the test report of HPLC measurement for samples with thicknesses of 6.9 and 0.7 μm. UVB-irradiated samples corresponded to retention times of 8.9 and 6 min for each standard sample. The variation of the peak areas is due to the thickness difference and sheet area difference during sampling. The difference in retention time was due to the difference in dilution rate between the samples measured on different days [24]. Figure 3d shows the measured HPLC data with retention time of 8.941 min and area of 2795.98 mAU·s, which is the representative sample with the highest peak (Sample 2). As a result, it can be seen that vitamins are formed after UVB exposure; this is confirmed by detection in the standard sample with the same retention time. On the contrary, small peaks were detected in samples with low thickness. However, the vitamin D<sub>3</sub> observed in the film may be part of the vitamin D<sub>3</sub> converted from previtamin D<sub>3</sub>. This is because the complete coated 7-DHC and PMMA films may not have been subjected to the UVB irradiation or heating processes.

**Table 1.** Test report of HPLC for samples.

Sample Type	Sample No.	Ret. Time (min)	Width (min)	Area (mAU·s)	Height (mAU)
High	1	8.953	0.3007	2239.23169	115.23065
	2	8.941	0.2474	2795.98169	172.19246
	3	8.907	0.2928	1584.80652	82.99876
	4	8.908	0.2442	2566.54590	159.08534
Low	6	5.933	0.1580	9.45652	0.91976
	7	5.936	0.1661	27.24610	2.44307
	8	5.945	0.1684	42.18789	3.77591
	9	5.951	0.1650	41.45271	3.80933
	10	5.959	0.1661	38.68693	3.52437

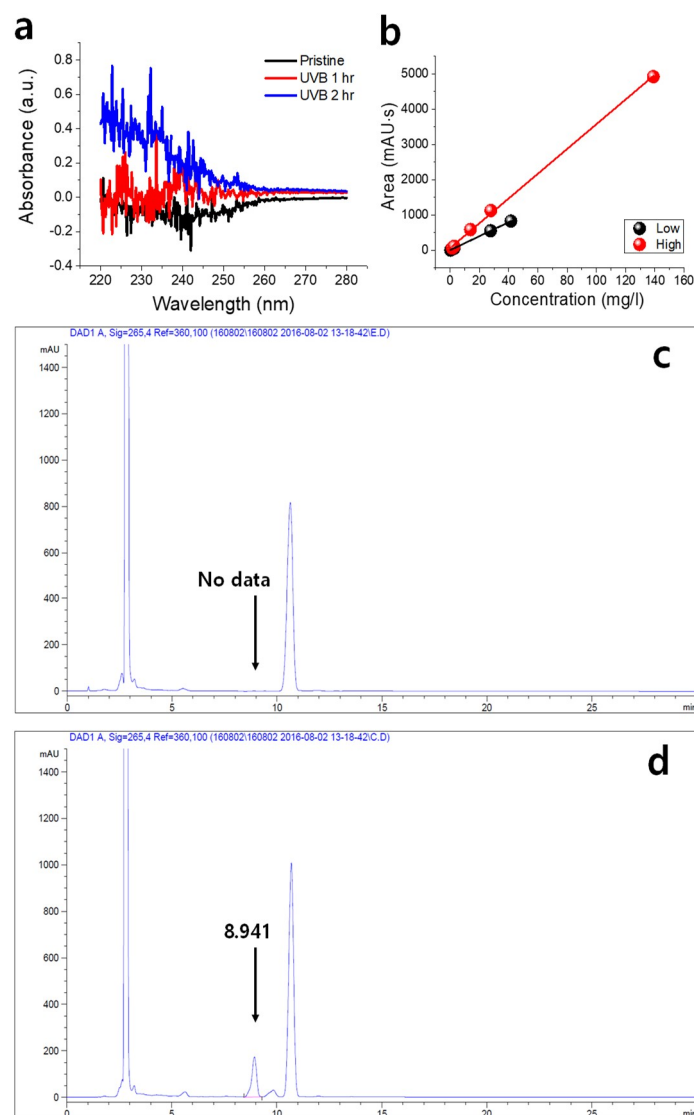


**Figure 3.** Characterizations for confirmation of previtamin D<sub>3</sub>. (a) The variation of the absorbance data with the polyethylene terephthalate (PET) substrate. (b) The area of the standard vitamin D<sub>3</sub> sample in high-performance liquid chromatography (HPLC) was changed according to the concentration and showed linearity. HPLC data of 7-DHC/PMMA samples (c) without and (d) with post-treatment (UVB irradiation and heating). A significant peak can be observed after post-treatment, suggesting the formation of vitamin D<sub>3</sub>. Figure S4 shows a photograph of the prepared samples.

The actual vitamin D<sub>3</sub> concentration in the samples can be obtained, as shown in Figure 4a, by using the calibration curves shown in Figure 3b. The vitamin D<sub>3</sub> concentrations were obtained as  $127 \pm 30$  and  $1.42 \pm 0.7$  mg/L at thicknesses of 6.9 and 0.7  $\mu\text{m}$ , respectively. This value is ~0.5–43% that of oral vitamin D<sub>3</sub>. As mentioned earlier, this is not a low amount because vitamin D<sub>3</sub> formed from 7-DHC is more effective than that obtained through oral nutrients. Figure 4b shows the amount of vitamin D<sub>3</sub> that was generated from the 7-DHC film. The previously prepared sample had area of 120 mm  $\times$  30 mm and multiplying it by the coated thickness gives the volume of each sample. The obtained amount of vitamin D<sub>3</sub> in high- and low-thickness samples was  $3.16 \pm 0.746$  mg and  $3 \pm 2$   $\mu\text{g}$ , respectively. This value was obtained from 7-DHC amounts of  $24.8 \pm 1.44$  and  $2.52 \pm 1.08$  mg, respectively, contained in the specific volume before UVB irradiation. The rate of conversion of 7-DHC to vitamin D<sub>3</sub> was 12.7% in a thick sample; this is much higher than the rate of 0.24% seen in a low-thickness sample. The low rate in the low-thickness samples is attributed to environmental factors such as air and moisture acting on the outer layer.

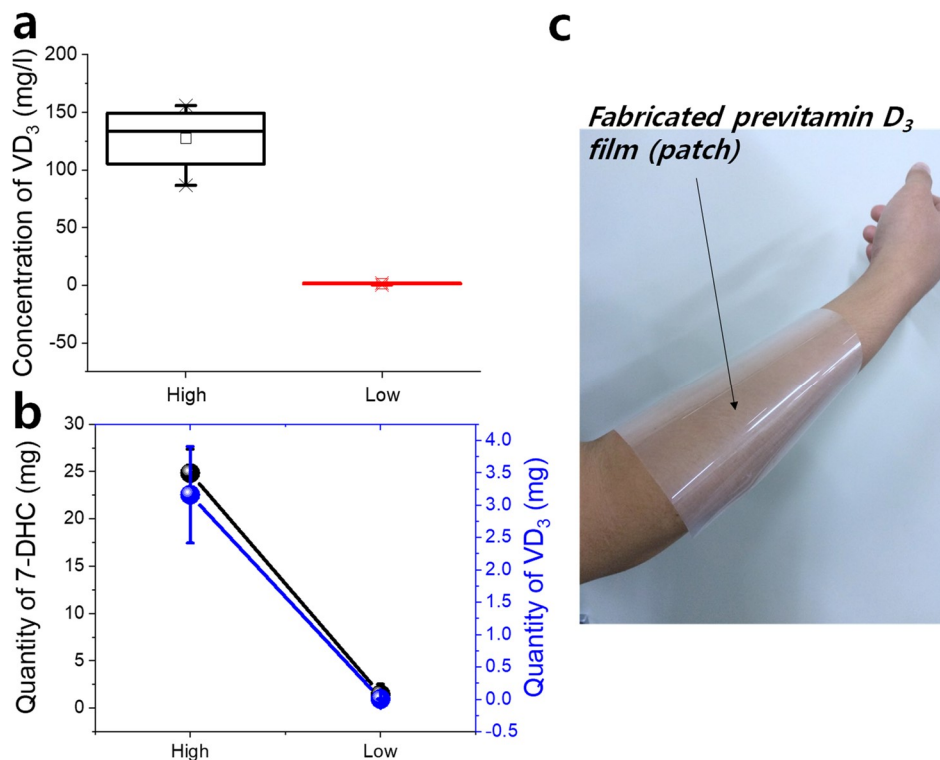


**Figure 4.** Quantitative calculation of the obtained vitamin  $D_3$ . (a) Comparison by layer thickness and (b) with 7-DHC by thickness of specific area of the film. (c) Conceptual photograph showing the use of the previtamin  $D_3$  film (V-Skin).

### 3. Conclusions

This study proposes a novel R2R process for manufacturing previtamin  $D_3$  films. The main concept in the proposed method is the mechanism of photoconversion of provitamin  $D_3$  to previtamin  $D_3$  and thermal isomerization of vitamin  $D_3$ . The human epidermis is mimicked by a PMMA-mixed 7-DHC layer on a flexible substrate that serves as the previtamin  $D_3$  patch; this product is called V-Skin (Figure 4c). The blends were coated using an R2R slot-die coating process and dried with a FIR lamp. Moreover, the UVB lamp helps to convert the coated film into a previtamin  $D_3$  layer. Here, we confirmed the presence of vitamin  $D_3$  by HPLC measurement. The HPLC profile clearly showed the standard sample of vitamin  $D_3$  from the UVB-irradiated samples. This study can serve as a meaningful basic study that can help overcome the problems of low efficacy of oral vitamin  $D_3$ , lack of sunshine, the harmfulness of ultraviolet rays, and indoor living for extended periods. In future studies, drug release and a clinical demonstration should be investigated to check the 25-OH-VitD level in the blood [25]. In this study, we focused on proposing and verifying a concept for mass production. This study should also lay the groundwork for future patch production through R2R-based drug film transfer.

### 4. Materials and Method

The coating solution was synthesized by mixing 1 wt.% 7-DHC [ $C_{27}H_{44}O$ , Sigma-Aldrich Co., LLC., Saint Louis, MO, USA], 18 wt.% PMMA [ $[CH_2C(CH_3)(CO_2CH_3)]_n$ , average Mw: ~120,000, Sigma-Aldrich Co., LLC.], 8.1 wt.% ethanol [ $CH_3CH_2OH$ , Sigma-Aldrich Co., LLC.], and 72.9 wt.% acetone [ $CH_3COCH_3$ , Sigma-Aldrich Co., LLC.]. For lab-scale validation, the coating solution was coated on a sapphire substrate with increasing spinning velocity up to 3000 rpm by using a commercial spin coater (ACE-2000, Dong Ah Trade Corp Co., Ltd., Seoul, Korea). The coated layer was dried at 60 °C for 30 min in a vacuum oven. Subsequently, a piece of the coated substrate was irradiated by a UVB lamp (TL T12 40W/01 RS UVB, Philips Inc., Amsterdam, The Netherlands) in a darkroom. The absorbance of the coated layer was measured using a UV/Vis spectrophotometer (Optizen 2120

UV, Mecasys Co., Ltd., Daejeon, Korea). In the R2R experiment, a slot-die coater (Naraenanotech Co., Ltd., Yongin, Korea) was used to obtain coating width of up to 130 mm. The PET films used had a width of 150 mm and a thickness of 100  $\mu\text{m}$  (SH-34, SKC Co., Ltd., Seoul, Korea). The operating tension was set to 10 N, the coating gap was 100  $\mu\text{m}$ , and the printing velocity varied from 1 to 6 m/min. The 7-DHC coated layer was dried at 60  $^{\circ}\text{C}$  through the dryer length of 18 m and was rewound. The coated thickness was measured using an interferometer (NV-2000, Nanosystems Co., Ltd., Daejeon, Korea). HPLC results were obtained using the 1260 Infinity HPLC device (Agilent Technologies Inc., Santa Clara, CA, USA). The column used, column temperature, mobile phase, flow rate, detector, and injection amount were Eclipse XDE C18 (4.6 mm  $\times$  250 mm  $\times$  5  $\mu\text{m}$ ), 40  $^{\circ}\text{C}$ , isocratic (acetonitrile:methanol = 6:4), 1 mL/min, diode array detector (265 nm), and 10  $\mu\text{L}$ , respectively. The measurements were performed at the Korea Polymer Testing and Research Institute (KOPTRI, Seoul), Ltd., an internationally recognized measurement institute.

**Supplementary Materials:** The following are available online at <http://www.mdpi.com/2079-6412/9/9/577/s1>, Figure S1: A photograph of the R2R system and the fabrication of 7-DHC/PMMA-coated films, Figure S2: The estimated thickness of the slot-die coating process, Figure S3: Schematic of the 7-DHC/PMMA film on PET substrate using UV/Vis spectrophotometer, Figure S4: Photographs of the prepared samples: (a) standard and (b) experiment, Figure S5: HPLC data of standard sample of high-thickness layers: (a) standard sample, (b) sample 0 (without UVB irradiation), (c) sample 1, (d) sample 2, (e) sample 3, and (f) sample 4, Figure S6: HPLC data of standard sample of low-thickness layers: (a) standard sample, (b) sample 6, (c) sample 7, (d) sample 8, (e) sample 9, and (f) sample 10, Table S1: The operation conditions of R2R slot-die coating, Table S2: HPLC of commercial vitamin D<sub>3</sub>.

**Author Contributions:** Conceptualization: K.-H.S. and D.L.; Data curation: J.P., Y.M., J.L., H.J. and Y.N.; Methodology: J.P., Y.M. and D.L.; Writing—original draft: J.P., Y.M. and D.L.; Writing—review and editing: J.P., K.-H.S. and D.L.

**Funding:** This work was supported by the Basic Science Research Program (2015R1C1A1A02037326) through the National Research Foundation of Korea (NRF) funded by the Ministry of Science, ICT and Future Planning. It was also supported by the Korea Institute of Energy Technology Evaluation and Planning (KETEP) and the Ministry of Trade, Industry and Energy (MOTIE) of the Korea (No. 20174010201490). Finally, this paper was supported by the Konkuk University Researcher Fund in 2018.

**Conflicts of Interest:** The authors declare no conflict of interest.

## References

1. Palacios, C.; Gonzalez, L. Is vitamin D deficiency a major global public health problem? *J. Steroid Biochem. Mol. Biol.* **2014**, *144*, 138–145. [[CrossRef](#)] [[PubMed](#)]
2. Webb, A.R.; Holick, M.F. The role of sunlight in the cutaneous production of vitamin D<sub>3</sub>. *Annu. Rev. Nutr.* **1988**, *8*, 375–399. [[CrossRef](#)] [[PubMed](#)]
3. Holick, M.F.; Chen, T.C. Vitamin D deficiency: A worldwide problem with health consequences. *Am. J. Clin. Nutr.* **2008**, *87*, 1080S–1086S. [[CrossRef](#)] [[PubMed](#)]
4. Buttriss, J.L. Vitamin D: Sunshine vs. diet vs. pills. *Nutr. Bull.* **2015**, *40*, 279–285. [[CrossRef](#)]
5. De Gruijl, F.R.; van Kranen, H.J.; Mullenders, L.H. UV-induced DNA damage, repair, mutations and oncogenic pathways in skin cancer. *J. Photochem. Photobiol. B Biol.* **2001**, *63*, 19–27. [[CrossRef](#)]
6. Sharma, S.; Barr, A.B.; Macdonald, H.M.; Sheehy, T.; Novotny, R.; Corriveau, A. Vitamin D deficiency and disease risk among aboriginal Arctic populations. *Nutr. Rev.* **2011**, *69*, 468–478. [[CrossRef](#)] [[PubMed](#)]
7. Kim, S.H.; Youn, J.Y.; Kim, K.M.; Kang, K.C.; Pyo, H.B.; Lee, S.J. Characterization of an inclusion complex of 7-dehydrocholesterol and cyclodextrin. *J. Ind. Eng. Chem.* **2010**, *16*, 119–121. [[CrossRef](#)]
8. Lee, J.; Park, J.; Jeong, H.; Shin, K.-H.; Lee, D. Optimization of printing conditions for microscale multiline printing in continuous roll-to-roll gravure printing. *J. Ind. Eng. Chem.* **2016**, *42*, 131–141. [[CrossRef](#)]
9. Galkin, O.N.; Terenetskaya, I.P. Vitamin D<sup>3</sup> biosimeter: Basic characteristics and potential applications. *J. Photochem. Photobiol. B Biol.* **1999**, *53*, 12–19. [[CrossRef](#)]
10. Jacobs, H.J.C.; Havinga, E. Photochemistry of vitamin D and its isomers and of simple trienes. *Adv. Photochem.* **1979**, *11*, 305–373.
11. Terenetskaya, I.P. Provitamin D photoisomerization as possible UV-B monitor: Kinetic study using tunable dye-laser. *Laser-Tissue Interact. V Ultrav. Radiat. Hazards* **1994**, *2134*, 135–140.

12. Norman, A.W. Sunlight, season, skin pigmentation, vitamin D, and 25-hydroxyvitamin D: Integral components of the vitamin D endocrine system. *Am. J. Clin. Nutr.* **1998**, *68*, 1108–1110. [[CrossRef](#)] [[PubMed](#)]
13. Terenetska, I.P.; Orlova, T.M.; Kirilenko, E.K.; Galich, G.A.; Eremneko, A.M. Methods and Devices for in situ Determination of a Vitamin-D Synthesizing Amount of Natural and Artificial UV Irradiation. U.S. Patent 8,552,391, 8 October 2013.
14. Krebs, F.C.; Tromholt, T.; Jørgensen, M. Upscaling of polymer solar cell fabrication using full roll-to-roll processing. *Nanoscale* **2010**, *2*, 873–886. [[CrossRef](#)] [[PubMed](#)]
15. Park, J.; Lee, J.; Noh, Y.; Shin, K.-H.; Lee, D. Flexible ultraviolet photodetectors with ZnO nanowire networks fabricated by large area controlled roll-to-roll processing. *J. Mater. Chem. C* **2016**, *4*, 7948–7958. [[CrossRef](#)]
16. Park, J.; Shin, K.; Lee, C. Roll-to-roll coating technology and its applications: A review. *Int. J. Precis. Eng. Manuf.* **2016**, *17*, 537–550. [[CrossRef](#)]
17. Carvalho, M.S.; Khesghi, H.S. Low-flow limit in slot coating: Theory and experiments. *AIChE J.* **2000**, *46*, 1907–1917. [[CrossRef](#)]
18. Krebs, F.C. Fabrication and processing of polymer solar cells: A review of printing and coating techniques. *Sol. Energy Mater. Sol. Cells* **2009**, *93*, 394–412. [[CrossRef](#)]
19. Kang, H.; Park, J.; Shin, K. Statistical analysis for the manufacturing of multi-strip patterns by roll-to-roll single slot-die systems. *Robot. Comput. Integr. Manuf.* **2014**, *30*, 363–368. [[CrossRef](#)]
20. Park, J.; Shin, K.; Lee, C. Optimized design for anti-reflection coating process in roll-to-roll slot-die coating system. *Robot. Comput. Integr. Manuf.* **2014**, *30*, 432–441. [[CrossRef](#)]
21. Romero, O.; Scriven, L.; Carvalho, M. Slot coating of mildly viscoelastic liquids. *J. Non-Newton. Fluid Mech.* **2006**, *138*, 63–75. [[CrossRef](#)]
22. Yang, L.; Zhai, Q.; Li, G.; Jiang, H.; Han, L.; Wang, J.; Wang, E. A light transmission technique for pore size measurement in track-etched membranes. *Chem. Commun.* **2013**, *49*, 11415–11417. [[CrossRef](#)] [[PubMed](#)]
23. Israeli-Lev, G.; Livney, Y.D. Self-assembly of hydrophobin and its co-assembly with hydrophobic nutraceuticals in aqueous solutions: Towards application as delivery systems. *Food Hydrocoll.* **2014**, *35*, 28–35. [[CrossRef](#)]
24. Abraham, E. A potential tissue culture approach for the phytoremediation of dyes in aquaculture industry. *Biochem. Eng. J.* **2016**, *115*, 23–29.
25. Osmancevic, A.; Sandström, K.; Gillstedt, M.; Landin-Wilhelmsen, K.; Larkö, O.; Larkö, A.-M.W.; Holick, M.F.; Krogstad, A.-L. Vitamin D production after UVB exposure—A comparison of exposed skin regions. *J. Photochem. Photobiol. B Biol.* **2015**, *143*, 38–43. [[CrossRef](#)] [[PubMed](#)]



© 2019 by the authors. Licensee MDPI, Basel, Switzerland. This article is an open access article distributed under the terms and conditions of the Creative Commons Attribution (CC BY) license (<http://creativecommons.org/licenses/by/4.0/>).